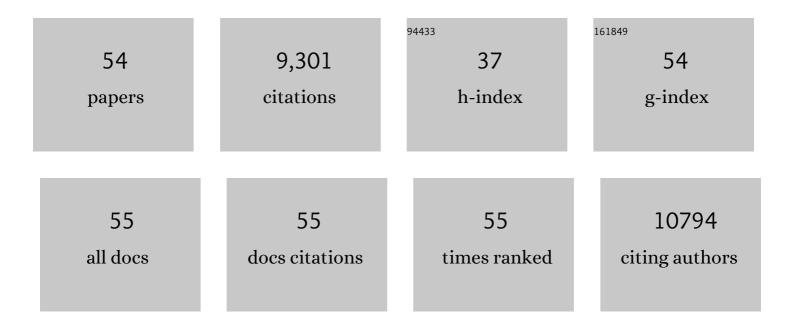
## Wenguang Tu

List of Publications by Year in descending order

Source: https://exaly.com/author-pdf/2778265/publications.pdf Version: 2024-02-01



WENCHANG TH

#	Article	IF	CITATIONS
1	Host/Guest Nanostructured Photoanodes Integrated with Targeted Enhancement Strategies for Photoelectrochemical Water Splitting. Advanced Science, 2022, 9, e2103744.	11.2	31
2	Single Pd–S <i><sub>x</sub></i> Sites <i>In Situ</i> Coordinated on CdS Surface as Efficient Hydrogen Autotransfer Shuttles for Highly Selective Visible-Light-Driven C–N Coupling. ACS Catalysis, 2022, 12, 4481-4490.	11.2	28
3	New black indium oxide—tandem photothermal CO2-H2 methanol selective catalyst. Nature Communications, 2022, 13, 1512.	12.8	47
4	Shedding light on <scp>CO<sub>2</sub></scp> : Catalytic synthesis of solar methanol. EcoMat, 2021, 3, e12078.	11.9	13
5	Single-Ni Sites Embedded in Multilayer Nitrogen-Doped Graphene Derived from Amino-Functionalized MOF for Highly Selective CO <sub>2</sub> Electroreduction. ACS Sustainable Chemistry and Engineering, 2021, 9, 3792-3801.	6.7	24
6	Hollow InVO <sub>4</sub> Nanocuboid Assemblies toward Promoting Photocatalytic N <sub>2</sub> Conversion Performance. Advanced Materials, 2021, 33, e2006780.	21.0	38
7	Manipulating Intermediates at the Au–TiO <sub>2</sub> Interface over InP Nanopillar Array for Photoelectrochemical CO <sub>2</sub> Reduction. ACS Catalysis, 2021, 11, 11416-11428.	11.2	48
8	In Situ Determination of Polaron-Mediated Ultrafast Electron Trapping in Rutile TiO <sub>2</sub> Nanorod Photoanodes. Journal of Physical Chemistry Letters, 2021, 12, 10815-10822.	4.6	14
9	Rational Synthesis of Amorphous Ironâ€Nickel Phosphonates for Highly Efficient Photocatalytic Water Oxidation with Almost 100 % Yield. Angewandte Chemie - International Edition, 2020, 59, 1171-1175.	13.8	32
10	Rational Synthesis of Amorphous Ironâ€Nickel Phosphonates for Highly Efficient Photocatalytic Water Oxidation with Almost 100 % Yield. Angewandte Chemie, 2020, 132, 1187-1191.	2.0	4
11	Isolated Ni single atoms in nitrogen doped ultrathin porous carbon templated from porous g-C3N4 for high-performance CO2 reduction. Nano Energy, 2020, 77, 105158.	16.0	83
12	Ultralow-temperature assisted synthesis of single platinum atoms anchored on carbon nanotubes for efficiently electrocatalytic acidic hydrogen evolution. Journal of Energy Chemistry, 2020, 51, 280-284.	12.9	84
13	Anchoring Active Pt <sup>2+</sup> /Pt <sup>0</sup> Hybrid Nanodots on g <sub>3</sub> N <sub>4</sub> Nitrogen Vacancies for Photocatalytic H <sub>2</sub> Evolution. ChemSusChem, 2019, 12, 2029-2034.	6.8	54
14	The pulsed laser-induced Schottky junction via in-situ forming Cd clusters on CdS surfaces toward efficient visible light-driven photocatalytic hydrogen evolution. Applied Catalysis B: Environmental, 2019, 258, 117967.	20.2	148
15	Isolated Squareâ€Planar Copper Center in Boron Imidazolate Nanocages for Photocatalytic Reduction of CO <sub>2</sub> to CO. Angewandte Chemie, 2019, 131, 11878-11882.	2.0	32
16	Construction of holeâ€transported MoO <sub>3â€<i>x</i></sub> coupled with CdS nanospheres for boosting photocatalytic performance via oxygenâ€defectsâ€mediated Zâ€scheme charge transfer. Applied Organometallic Chemistry, 2019, 33, e4780.	3.5	29
17	MOF-derived hierarchical hollow spheres composed of carbon-confined Ni nanoparticles for efficient CO <sub>2</sub> methanation. Catalysis Science and Technology, 2019, 9, 731-738.	4.1	87
18	Isolated Squareâ€Planar Copper Center in Boron Imidazolate Nanocages for Photocatalytic Reduction of CO <sub>2</sub> to CO. Angewandte Chemie - International Edition, 2019, 58, 11752-11756.	13.8	194

#	Article	IF	CITATIONS
19	Effects of composition faults in ternary metal chalcogenides (Zn In2S3+, x = 1–5) layered crystals for visible-light-driven catalytic hydrogen generation and carbon dioxide reduction. Applied Catalysis B: Environmental, 2019, 256, 117810.	20.2	82
20	Electrical promotion of spatially photoinduced charge separation via interfacial-built-in quasi-alloying effect in hierarchical Zn2ln2S5/Ti3C2(O, OH)x hybrids toward efficient photocatalytic hydrogen evolution and environmental remediation. Applied Catalysis B: Environmental, 2019, 245, 290-301.	20.2	229
21	Tailored indium sulfide-based materials for solar-energy conversion and utilization. Journal of Photochemistry and Photobiology C: Photochemistry Reviews, 2019, 38, 1-26.	11.6	127
22	Formation of quasi-core-shell In2S3/anatase TiO2@metallic Ti3C2Tx hybrids with favorable charge transfer channels for excellent visible-light-photocatalytic performance. Applied Catalysis B: Environmental, 2018, 233, 213-225.	20.2	297
23	Photogenerated charge transfer via interfacial internal electric field for significantly improved photocatalysis in direct Z-scheme oxygen-doped carbon nitrogen/CoAl-layered double hydroxide heterojunction. Applied Catalysis B: Environmental, 2018, 227, 530-540.	20.2	219
24	Template-Induced High-Crystalline g-C <sub>3</sub> N <sub>4</sub> Nanosheets for Enhanced Photocatalytic H <sub>2</sub> Evolution. ACS Energy Letters, 2018, 3, 514-519.	17.4	259
25	Quasi-polymeric construction of stable perovskite-type LaFeO3/g-C3N4 heterostructured photocatalyst for improved Z-scheme photocatalytic activity via solid p-n heterojunction interfacial effect. Journal of Hazardous Materials, 2018, 347, 412-422.	12.4	296
26	Construction of hierarchical 2D-2D Zn3In2S6/fluorinated polymeric carbon nitride nanosheets photocatalyst for boosting photocatalytic degradation and hydrogen production performance. Applied Catalysis B: Environmental, 2018, 233, 58-69.	20.2	213
27	A Highly Efficient Oxygen Evolution Catalyst Consisting of Interconnected Nickel–Iron‣ayered Double Hydroxide and Carbon Nanodomains. Advanced Materials, 2018, 30, 1705106.	21.0	209
28	Premixed Stagnation Flame Synthesized TiO <sub>2</sub> Nanoparticles with Mixed Phases for Efficient Photocatalytic Hydrogen Generation. ACS Sustainable Chemistry and Engineering, 2018, 6, 14470-14479.	6.7	25
29	Aminoâ€Assisted Anchoring of CsPbBr <sub>3</sub> Perovskite Quantum Dots on Porous gâ€C <sub>3</sub> N <sub>4</sub> for Enhanced Photocatalytic CO <sub>2</sub> Reduction. Angewandte Chemie, 2018, 130, 13758-13762.	2.0	172
30	Aminoâ€Assisted Anchoring of CsPbBr <sub>3</sub> Perovskite Quantum Dots on Porous gâ€C <sub>3</sub> N <sub>4</sub> for Enhanced Photocatalytic CO <sub>2</sub> Reduction. Angewandte Chemie - International Edition, 2018, 57, 13570-13574.	13.8	432
31	Visible-light-driven removal of tetracycline antibiotics and reclamation of hydrogen energy from natural water matrices and wastewater by polymeric carbon nitride foam. Water Research, 2018, 144, 215-225.	11.3	481
32	Rational Design of Catalytic Centers in Crystalline Frameworks. Advanced Materials, 2018, 30, e1707582.	21.0	103
33	Nickel Nanoparticles Encapsulated in Few‣ayer Nitrogenâ€Doped Graphene Derived from Metal–Organic Frameworks as Efficient Bifunctional Electrocatalysts for Overall Water Splitting. Advanced Materials, 2017, 29, 1605957.	21.0	507
34	Highly Efficient Solarâ€Driven Photothermal Performance in Au arbon Core‧hell Nanospheres. Solar Rrl, 2017, 1, 1600032.	5.8	24
35	Construction of unique two-dimensional MoS <sub>2</sub> –TiO <sub>2</sub> hybrid nanojunctions: MoS <sub>2</sub> as a promising cost-effective cocatalyst toward improved photocatalytic reduction of CO <sub>2</sub> to methanol. Nanoscale, 2017, 9, 9065-9070.	5.6	134
36	Unique PCoN Surface Bonding States Constructed on g <sub>3</sub> N <sub>4</sub> Nanosheets for Drastically Enhanced Photocatalytic Activity of H <sub>2</sub> Evolution. Advanced Functional Materials, 2017, 27, 1604328.	14.9	329

Wenguang Tu

#	Article	IF	CITATIONS
37	Constructing noble-metal-free Z-scheme photocatalytic overall water splitting systems using MoS <sub>2</sub> nanosheet modified CdS as a H <sub>2</sub> evolution photocatalyst. Journal of Materials Chemistry A, 2017, 5, 21205-21213.	10.3	92
38	Phosphonate-Based Metal–Organic Framework Derived Co–P–C Hybrid as an Efficient Electrocatalyst for Oxygen Evolution Reaction. ACS Catalysis, 2017, 7, 6000-6007.	11.2	149
39	Investigating the Role of Tunable Nitrogen Vacancies in Graphitic Carbon Nitride Nanosheets for Efficient Visible-Light-Driven H <sub>2</sub> Evolution and CO <sub>2</sub> Reduction. ACS Sustainable Chemistry and Engineering, 2017, 5, 7260-7268.	6.7	322
40	Fabrication of Oxygenâ€Đoped Double‣helled GaN Hollow Spheres toward Efficient Photoreduction of CO <sub>2</sub> . Particle and Particle Systems Characterization, 2016, 33, 583-588.	2.3	13
41	Photocatalytic reduction of CO <sub>2</sub> over Ag/TiO <sub>2</sub> nanocomposites prepared with a simple and rapid silver mirror method. Nanoscale, 2016, 8, 11870-11874.	5.6	139
42	Microstructure modulation of the CH3NH3PbI3 layer in perovskite solar cells by 2-propanol pre-wetting and annealing in a spray-assisted solution process. Journal of Materials Chemistry A, 2016, 4, 11372-11380.	10.3	17
43	Stateâ€ofâ€theâ€Art Progress in Diverse Heterostructured Photocatalysts toward Promoting Photocatalytic Performance. Advanced Functional Materials, 2015, 25, 998-1013.	14.9	706
44	Au@TiO <sub>2</sub> yolk–shell hollow spheres for plasmon-induced photocatalytic reduction of CO <sub>2</sub> to solar fuel via a local electromagnetic field. Nanoscale, 2015, 7, 14232-14236.	5.6	153
45	Hollow spheres consisting of Ti <sub>0.91</sub> O <sub>2</sub> /CdS nanohybrids for CO <sub>2</sub> photofixation. Chemical Communications, 2015, 51, 13354-13357.	4.1	71
46	Double-shelled plasmonic Ag-TiO2 hollow spheres toward visible light-active photocatalytic conversion of CO2 into solar fuel. APL Materials, 2015, 3, .	5.1	59
47	Photoconversion: Photocatalytic Conversion of CO <sub>2</sub> into Renewable Hydrocarbon Fuels: Stateâ€ofâ€theâ€Art Accomplishment, Challenges, and Prospects (Adv. Mater. 27/2014). Advanced Materials, 2014, 26, 4598-4598.	21.0	7
48	Formation of 3D interconnectively macro/mesoporous TiO <sub>2</sub> sponges through gelation of lotus root starch toward CO <sub>2</sub> photoreduction into hydrocarbon fuels. RSC Advances, 2014, 4, 43172-43177.	3.6	15
49	Photocatalytic Conversion of CO <sub>2</sub> into Renewable Hydrocarbon Fuels: Stateâ€ofâ€theâ€Art Accomplishment, Challenges, and Prospects. Advanced Materials, 2014, 26, 4607-4626.	21.0	1,319
50	An In Situ Simultaneous Reductionâ€Hydrolysis Technique for Fabrication of TiO <sub>2</sub> â€Graphene 2D Sandwichâ€Like Hybrid Nanosheets: Grapheneâ€Promoted Selectivity of Photocatalyticâ€Driven Hydrogenation and Coupling of CO <sub>2</sub> into Methane and Ethane. Advanced Functional Materials, 2013, 23, 1743-1749.	14.9	357
51	Versatile Grapheneâ€Promoting Photocatalytic Performance of Semiconductors: Basic Principles, Synthesis, Solar Energy Conversion, and Environmental Applications. Advanced Functional Materials, 2013, 23, 4996-5008.	14.9	335
52	Direct Growth of Fe <sub>2</sub> V <sub>4</sub> O <sub>13</sub> Nanoribbons on a Stainless‧teel Mesh for Visibleâ€Light Photoreduction of CO <sub>2</sub> into Renewable Hydrocarbon Fuel and Degradation of Gaseous Isopropyl Alcohol. ChemPlusChem, 2013, 78, 274-278.	2.8	41
53	Instant, template-free and fluorine-free synthesis of TiO2 nanotube arrays with a room-temperature solid–liquid arc discharge technique. CrystEngComm, 2012, 14, 7583.	2.6	5
54	Robust Hollow Spheres Consisting of Alternating Titania Nanosheets and Graphene Nanosheets with High Photocatalytic Activity for CO <sub>2</sub> Conversion into Renewable Fuels. Advanced Functional Materials, 2012, 22, 1215-1221.	14.9	373